Protein NMR Spectroscopy

Supramolecular Organization and Functional Implications of K+ Channel Clusters in Membranes

*Koen M. Visscher, João Medeiros-Silva, Deni Mance, João P. G. L. M. Rodrigues,
Mark Daniëls, Alexandre M. J. J. Bonvin, Marc Baldus, and Markus Weingarth**
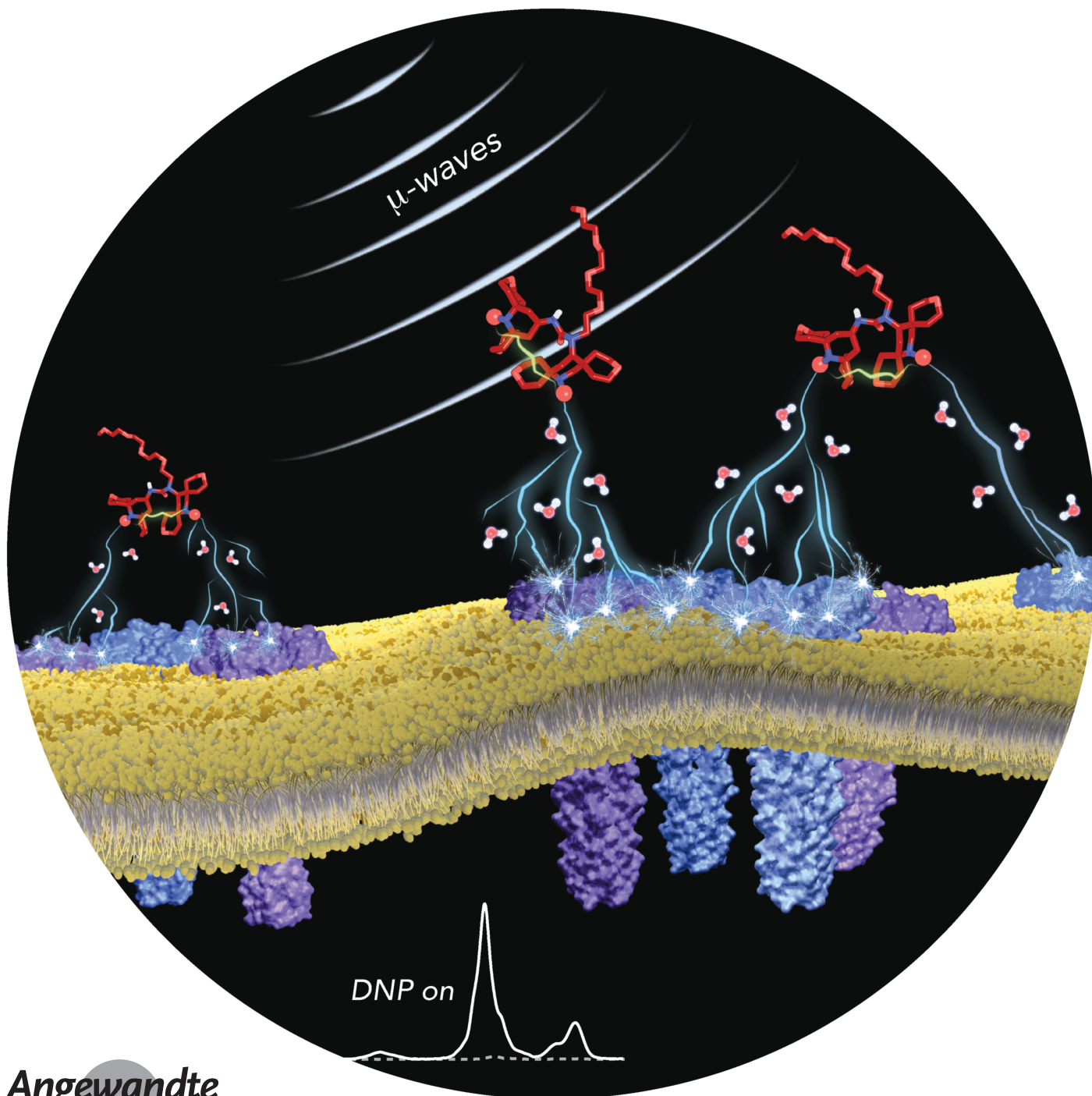
Abstract: The segregation of cellular surfaces in heterogeneous patches is considered to be a common motif in bacteria and eukaryotes that is underpinned by the observation of clustering and cooperative gating of signaling membrane proteins such as receptors or channels. Such processes could represent an important cellular strategy to shape signaling activity. Hence, structural knowledge of the arrangement of channels or receptors in supramolecular assemblies represents a crucial step towards a better understanding of signaling across membranes. We herein report on the supramolecular organization of clusters of the K^+ channel KcsA in bacterial membranes, which was analyzed by a combination of DNP-enhanced solid-state NMR experiments and MD simulations. We used solid-state NMR spectroscopy to determine the channel–channel interface and to demonstrate the strong correlation between channel function and clustering, which suggests a yet unknown mechanism of communication between K^+ channels.

Multiple lines of experimental evidence highlight the lateral patchiness of cellular surfaces, suggesting that membranes are organized in heterogeneous domains.[1] This corroborates the notion that membrane signaling proteins such as channels or receptors are assembled in supramolecular clusters, in which protein function is coupled,[2] possibly to achieve an optimal response to a single stimulus. Indeed, clustering and coupled gating have been reported for a number of ion channels, including mammalian K^+,[3] Na^+,[4] and Ca^{2+}[2b] channels. However, the principles of the arrangement of channel clusters and the implications of clustering for channel gating remain largely unknown.

KcsA is an archetypical K^+ channel and widely used to study ion channel gating. The KcsA pore is conserved across all K^+ channels and regulated by a cytoplasmic activation gate and an extracellular inactivation gate.[5] It has been demonstrated in vitro[6] and in vivo in *E. coli*[7] and in the native host *S. lividans*[8] that KcsA can form clusters. Herein, we have studied the supramolecular arrangement of KcsA clusters in *E. coli* membranes by conventional and dynamic nuclear polarization (DNP) enhanced solid-state NMR (ssNMR) experiments and coarse-grained molecular dynamics (CGMD) simulations. We demonstrate that KcsA channels assemble into clusters in native-like lipid membranes, and provide structural details on the channel–channel interface,

disclosing an unexpected role of a membrane-associated helix as a key element for clustering. Intriguingly, we demonstrate with DNP-ssNMR experiments that channel function and cluster formation are correlated, which suggests a thus far unknown mechanism of interchannel communication.

ssNMR spectroscopy provides a straightforward means for studying the clustering of membrane proteins by mixing proteins that carry different NMR-active nuclei X and Y (e.g., $X = {}^{15}N$ and $Y = {}^{13}C$).[9] Magnetization transfer between spin species X and Y necessitates the formation of clusters that are stable on the experimental timescale, which is in the range of µs to ms for dedicated dipolar transfer schemes.

We reconstituted an equimolar mixture of ^{15}N-labeled KcsA [U-^{15}N-KcsA] and ^{13}C-labeled KcsA [U-^{13}C-KcsA] in *E. coli* lipids at a 1:100 protein/lipid (P/L) molar ratio. We initially prepared the samples in neutral buffers (pH 7, 50 mм K^+), in which channels are in the closed–conductive gating mode, which we validated with a ssNMR 2D ^{13}C–^{13}C PARIS[10] spectrum (see the Supporting Information, Figure S1). In line with previous results,[11] the KcsA channels exhibited a parallel topology in this preparation (Figure S2). To probe KcsA clustering, we carried out a series of one-dimensional (1D) NHHC experiments,[9a] in which magnetization is initially created on ^{15}N nuclei (i.e., of U-^{15}N-KcsA) and transferred via short heteronuclear transfer steps and a longer ^1H–^1H dipolar mixing unit to ^{13}C nuclei (of U-^{13}C-KcsA; Figure 1A). We observed pronounced transfer to ^{13}C nuclei in the 1D NHHC spectra (Figure 1B), which strongly indicated the formation of KcsA clusters that are stable on the sub-millisecond timescale and probably beyond. As the ^1H-mediated magnetization transfer from ^{15}N to ^{13}C is short-ranged with an upper barrier of approximately 5 Å, the NHHC spectra strongly suggest that the clustered channels are in direct contact. Furthermore, while most of our ssNMR experiments were carried out at low temperature (at 255 K) for sensitivity reasons, cluster formation also occurred at higher temperature (293 K; Figure 1C). Note that magnetization transfer from ^{15}N to ^{13}C was virtually abolished in a mixture of U-^{15}N-KcsA and unlabeled KcsA, which means that putative spurious ^{13}C natural-abundance contributions can be neglected (Figure 1D), validating our setup. We would also like to emphasize that the homotetrameric KcsA is of outstanding stability in liposomes, and monomers dissociate neither at strongly elevated temperatures of 90°C[12] nor in harsh detergents such as SDS.[13] Therefore, signal intensity in NHHC experiments must result from contacts between different channels.

As a next step, we investigated if clustering correlates with KcsA function. It is currently not clear if or how clustering modulates KcsA function, and contradicting studies have been published in recent years. Molina and co-workers showed by electrophysiological measurements in liposomes that clustered channels open together in a concerted manner, and that clustering strongly increases channel open probability.[6a] However, in stark contrast to the studies by Molina and co-workers, AFM experiments, using truncated channels in zwitterionic lipids exposed to a mica surface, came to the conclusion that open channels do not form clusters.[6b] We tried to settle this striking conflict with a series of comparative

[*] K. M. Visscher, J. Medeiros-Silva, Dr. D. Mance,
Dr. J. P. G. L. M. Rodrigues, M. Daniëls, Prof. A. M. J. J. Bonvin,
Prof. M. Baldus, Dr. M. Weingarth
NMR Spectroscopy, Bijvoet Center for Biomolecular Research
Department of Chemistry, Utrecht University
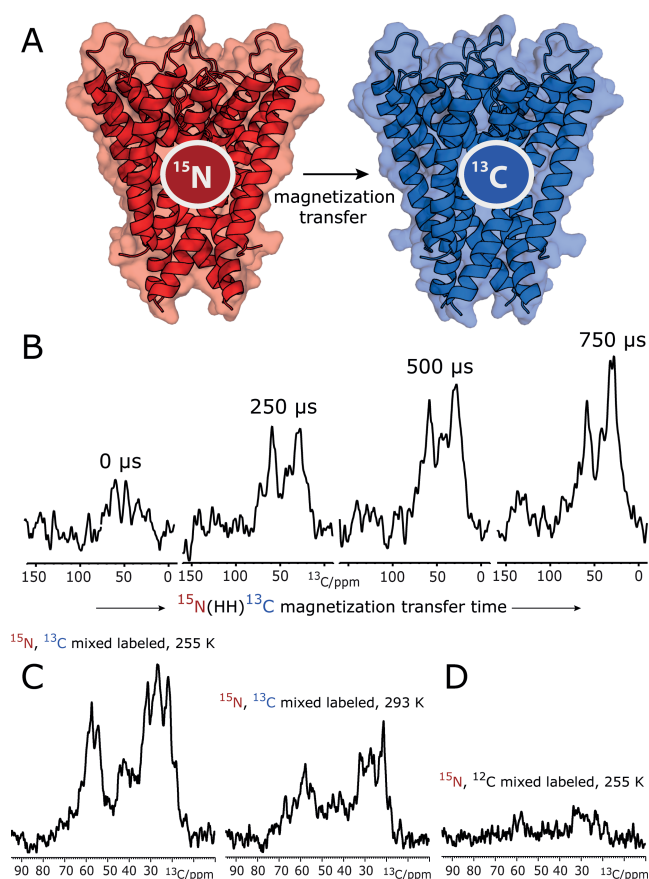Pandualaan 8, 3584 CH Utrecht (The Netherlands)
E-mail: M.H.Weingarth@uu.nl

Figure 1. ssNMR demonstrates that KcsA channels form clusters in *E. coli* lipids. A) KcsA clustering can be probed with an equimolar mixture of ¹⁵N- and ¹³C-labeled channels and dedicated ssNMR experiments such as NHHC.[9a] B) A series of 1D NHHC experiments with increasing ¹H–¹H magnetization transfer times applied to mixed-labeled channels show the presence of KcsA clusters. C) Cluster formation occurred at low (255 K) and high (293 K) temperature. The lower intensity at 293 K is due to increased local motion, which decreases the dipolar transfer efficiency. D) The virtual absence of signals without ¹³C labeling shows that natural-abundance contributions can be neglected.

1D NHHC measurements with closed and open full-length channels embedded in *E. coli* lipids. For these studies, it was critical to work at a low P/L ratio 1) to allocate enough space so that channels could potentially dissociate upon opening[6b] and 2) to exclude random channel–channel contacts. However, as a 1D NHHC experiment with a P/L ratio of 1:100 (Figure 1) already required a measurement time of about one day, substantially lower P/L ratios were prohibitive with conventional NMR spectroscopy. We overcame this issue with the DNP technique, which can provide sensitivity gains of two orders of magnitude, and thereby enables otherwise infeasible ssNMR experiments with lowly concentrated membrane proteins (for examples, see Refs. [9b,14]). We prepared vesicles with mixed ¹⁵N/¹³C-labeled channels and ran experiments using a 263 GHz/400 MHz DNP/ssNMR setup at 100 K (see also the Supporting Information). We obtained signal enhancement factors ε of 20–55, which are comparable to those in our previous DNP applications with KcsA.[14c] Importantly, this enhancement allowed us to work at

a much lower P/L ratio of 1:400, ensuring that the DNP-ssNMR results reflect specific channel–channel contacts in reference to the gating mode. We first conducted DNP-ssNMR experiments with closed channels (at pH 7), which confirmed the formation of clusters. Afterwards, we washed exactly the same sample in acidic (pH 4) buffers, which is a well-known means to open the activation gate of KcsA.[5,15,16] Unexpectedly, we obtained drastically increased NHHC transfer efficiencies with open channels (Figure 2 A). We confirmed this result by "shuttling" the channels back to the closed state (pH 7), for which the NHHC transfer was again much weaker (Figure 2 B). Hence, our DNP-ssNMR experiments in native bacterial lipids revealed that cluster formation is a reversible, dynamic process that is correlated with the gating cycle of KcsA. Moreover, our study unambiguously demonstrates that open channels form clusters, which explains previous results from Molina and co-workers.[6a] Furthermore, our study reveals that the opening of the activating gate strongly stimulates cluster formation.

But what causes the surprising increase in cluster formation upon channel opening, and how can clustered channels communicate to open simultaneously? Our data demonstrate that the channel–channel interface is modulated during the closed-to-open transition. This very strongly suggests that a structural element that is involved in channel opening is also involved in the channel–channel interface. The major structural event upon channel opening is a conformational change of the inner transmembrane (TM2) helix, and this unseals the cytoplasmic gate. However, it appears hardly possible that the TM2 helix, which is hidden in the interior of KcsA, contributes to channel–channel interactions. Another structural element that responds to the closed-to-open transition is the membrane-associated M0 helix, formed by the N-terminal residues M1–G21.[17] Indeed, it seems much more likely that M0 helices are involved in cluster formation, given that they are by far the most protruding element of the KcsA channel in the membrane plane.

Upon channel opening, in a mechanism dubbed "roll and stabilize", the M0 helix undergoes a major conformational change that buries hydrophobic M0 residues in the bilayer and exposes charged residues to lipid head groups.[17] The M0 helix could hence be a switch to modulate clustering, and we therefore hypothesized that these helices contribute to the channel–channel interface.

To investigate the channel–channel interface in further detail, we resorted to coarse-grained molecular dynamics (CGMD) simulations using the MARTINI force field.[18] Such simulations have both the long temporal and large spatial scale to study membrane protein clustering.[19] However, we would like to note that CGMD simulations only provide limited insight into cluster formation. First, such simulations are necessarily less accurate than all-atom simulations, and this may lead to an overestimation of intermolecular interactions. Second, the MARTINI force field is limited in its response to changes in the simulated environment, and secondary structure changes, for example, are not permitted. However, we would like to emphasize that overestimations of channel–channel interactions are of lesser concern, given that we have clearly demonstrated that KcsA forms clusters in
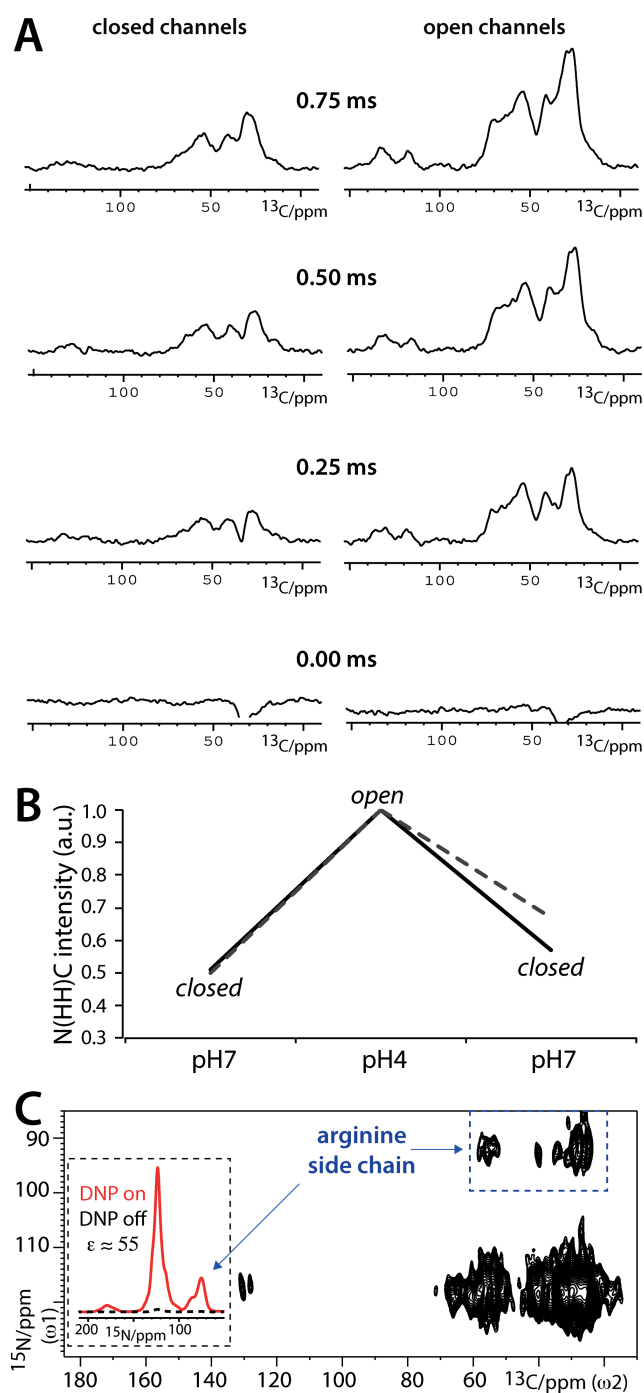
A

B

C

Figure 2. DNP-ssNMR experiments to probe KcsA clustering in reference to function. A) A series of 1D NHHC spectra for closed–conductive (left) and open–inactivated (right) mixed-labeled channels (see also Figure S4). Spectra are normalized (see the Supporting Information) and ordered according to the ^{1}H–^{1}H mixing time. B) Comparison of NHHC spectra measured with a ^{1}H–^{1}H mixing time of 0.75 ms. Spectra were normalized according to the highest intensity at the signal maxima at $\delta(^{13}C) = 27$ ppm (black continuous lines) and $\delta(^{13}C) = 54$ ppm (gray dashed lines). Note that the same sample was used for Figures 2 A–C. C) DNP-enhanced 2D NHHC spectrum, measured with mixed-labeled closed (pH 7) KcsA channels. The comparison of 1D ^{15}N cross-polarization spectra in the inset illustrates the DNP enhancement of 55. The blue dashed box marks the channel–channel contacts that involve arginine side chains. To save experimental time, the Arg signals at $\delta(^{15}N) \approx 75$ ppm were back-folded to $\delta(^{15}N) = 95$ ppm in the 2D NHHC spectrum.

membranes. Moreover, ssNMR studies of KcsA in *E. coli* membranes, in which KcsA forms clusters (Figures 1 and 2), show only minimal secondary-structure changes as compared to the crystal structures.[20] Finally, it is not realistic to study channel clustering with all-atom simulations on the relevant timescales.

We performed CGMD simulations in which 16 closed KcsA channels, derived from PDB No. 1K4C (comprising residues S22–H124), were initially equidistantly placed in a large membrane composed of 3280 DOPE, 944 DOPG, and 480 cardiolipin lipids, approximating the composition of the inner *E. coli* membrane.[21] The P/L ratio was approximately 1:300 (see the Supporting Information for simulation details). To probe the influence of the M0 helix on clustering, we simulated these channels in the absence and presence of this helix (Figure 3 A,B). For the latter case, the M0 helix was added with MODELLER. Each simulation was run for a total duration of 37.5 µs. Indeed, the simulations clearly showed that the M0 helices modulate clustering. In the absence of the M0 helix, only small dimeric or trimeric clusters formed. However, the presence of M0 helices much accelerated clustering, with M0 helices acting as flexible tentacles that initiate channel–channel contacts. Intriguingly, M0 helices of clustered channels cast a kind of elongated mesh of 40 nm width, in which channels are entangled and from which they cannot easily escape. Such large assemblies are in line with in vivo and in vitro measurements, which revealed large KcsA clusters of 50 nm width.[6b,8] Notably, channel–channel contacts are relatively dynamic in this mesh (see Movie S1), and this is likely necessary so that channel—channel interactions can respond to gating transitions (Figure 2). Note that we did not consider the cytoplasmic domain (CPD) of KcsA in the simulations as previous studies had shown that the CPD does not take part in clustering.[6a,b] In line with these findings, an alignment of full-length KcsA[22] to our model of clusters shows that the CPDs of clustered channels are far away from each other (Figure S3).

Importantly, the M0 helix also has a strong influence on the channel–channel interface. In the absence of this helix (Figure 3 C), the interface is dominated by the TM1 helix. As we had assumed, the inner TM2 helix does not contribute to the interface. In the presence of the M0 helices, the interface is dominated by the mutually interacting M0 helices, which sterically prevent the TM1 helix from taking part in clustering. Moreover the turret, which connects the TM1 to the selectivity filter, is also involved in the interface (Figure 3 D). We sought to corroborate our structural model with a 2D NHHC ssNMR experiment, which critically required DNP enhancement for sensitivity reasons. An enhancement of $\varepsilon = 55$ enabled the acquisition of a 2D NHHC spectrum in only three days (Figure 2 C). While the resolution of the backbone amino protons ($\delta(^{15}N) = 100$–130 ppm) in the 2D experiment did not permit the assignment of specific contacts, we observed very strong correlations characteristic for polarization transfer from the arginine guanidinium group (resonating at $\delta(^{15}N) = 75$–80 ppm) to ^{13}C atoms in the backbone and side chains. The strong arginine contribution at the interface strongly corroborates the presence of the M0 helix at the interface (Figure 3 D). Indeed, with the M0 helix, a total
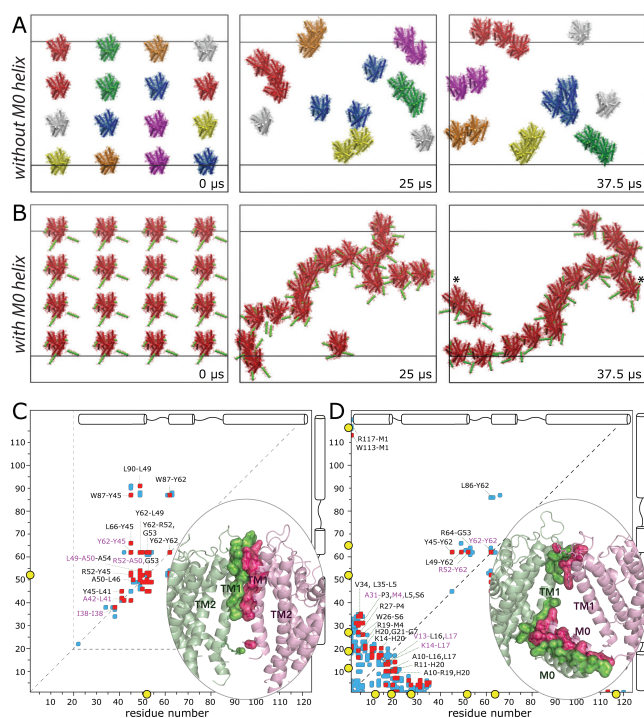
Figure 3. KcsA cluster formation probed by CGMD simulations. A) Evolution of channels without the M0 helix. Channels in the same clusters are shown in the same colors. B) Evolution of channels with the M0 helix, highlighted in green. Channels marked with asterisks form clusters over periodic boundaries. The snapshot after 37.5 μs was laterally translated by 5 nm. C, D) Contact maps derived from back-transformed[23] atomic-resolution interfaces sampled over the last 7.5 μs of the simulations. The maps show residue pairs of interacting channels within 5 Å distance without (C) and with (D) M0 helices. Pairs that were populated by >30% and <30% in comparison to the most populated pair are shown in red and blue, respectively. The five most populated pairs are shown in magenta. Pairs populated by <10% are not shown. Yellow circles highlight arginine residues at the interface. Representative high-resolution interfaces are shown in the bottom-right corners.

of six Arg residues (R11, R19, R27, R52, R64, R117) are heavily involved in channel–channel contacts. However, without the M0 helix (Figure 3 C), the interface is dominated by the hydrophobic TM1 helix, and only a single arginine (R52) contributes to interchannel contacts. Aside from this experimental evidence, it is sterically hardly possible that the protruding M0 helices are not present at the interface.

Note that the use of 800 MHz DNP[14c] would have provided little additional information in this study because its application would have been limited to 1D experiments for sensitivity reasons. Likewise, 2D or 3D experiments of the N(HH)CC type, which may provide precious information on the interface, were prohibited by the low spectral sensitivity in our strongly diluted membrane preparations.

In conclusion, we have dissected the anatomy of KcsA clusters in native bacterial lipids. By combining DNP-ssNMR experiments with MD simulations, we demonstrated that K+ channel gating and clustering are correlated in membranes, which hints at a relationship between KcsA localization and function. Thereby, our study solves a striking conflict[6b] in the

growing KcsA cluster literature, and strongly supports previous reports that KcsA channels can open in a concerted manner.[6a] Intriguingly, our study discloses that the membrane-associated M0 helix is a key element for cluster formation, and likely also for interchannel communication. In this context, our study highlights the importance of understanding how membrane proteins interact at high resolution, especially as protein assemblies are ubiquitous in crowded biological membranes.

Acknowledgements

Conflict of interest

The authors declare no conflict of interest.

[1] a) F. Spira, N. S. Mueller, G. Beck, P. von Olshausen, J. Beig, R. Wedlich-Soldner, *Nat. Cell Biol.* **2012**, *14*, 640–648; b) P. Sharma, R. Varma, R. C. Sarasij, Ira, K. Gousset, G. Krishna-moorthy, M. Rao, S. Mayor, *Cell* **2004**, *116*, 577–589.

[2] a) S. O. Marx, J. Gaburjakova, M. Gaburjakova, C. Henrikson, K. Ondrias, A. R. Marks, *Circ. Res.* **2001**, *88*, 1151–1158; b) M. F. Navedo, E. P. Cheng, C. Yuan, S. Votaw, J. D. Molkentin, J. D. Scott, L. F. Santana, *Circ. Res.* **2010**, *106*, 748–756; c) J. J. Sieber, K. I. Willig, C. Kutzner, C. Gerding-Reimers, B. Harke, G. Donnert, B. Rammner, C. Eggeling, S. W. Hell, H. Grubmuller, T. Lang, *Science* **2007**, *317*, 1072–1076.

[3] a) S. T. Lim, D. E. Antonucci, R. H. Scannevin, J. S. Trimmer, *Neuron* **2000**, *25*, 385–397; b) K. M. O'Connell, R. Loftus, M. M. Tamkun, *Proc. Natl. Acad. Sci. USA* **2010**, *107*, 12351–12356; c) Y. Horio, H. Hibino, A. Inanobe, M. Yamada, M. Ishii, Y. Tada, E. Satoh, Y. Hata, Y. Takai, Y. Kurachi, *J. Biol. Chem.* **1997**, *272*, 12885–12888.

[4] a) B. Naundorf, F. Wolf, M. Volgushev, *Nature* **2006**, *440*, 1060–1063; b) S. A. Freeman, A. Desmazieres, D. Fricker, C. Lubetzki, N. Sol-Foulon, *Cell. Mol. Life Sci.* **2016**, *73*, 723–735.

[5] G. Yellen, *Nature* **2002**, *419*, 35–42.

[6] a) M. L. Molina, F. N. Barrera, A. M. Fernandez, J. A. Poveda, M. L. Renart, J. A. Encinar, G. Riquelme, J. M. Gonzalez-Ros, *J. Biol. Chem.* **2006**, *281*, 18837–18848; b) A. Sumino, D. Yamamoto, M. Iwamoto, T. Dewa, S. Oiki, *J. Phys. Chem. Lett.* **2014**, *5*, 578–584; c) M. Yanagisawa, M. Iwamoto, A. Kato, K. Yoshikawa, S. Oiki, *J. Am. Chem. Soc.* **2011**, *133*, 11774–11779.

[7] A. M. Giudici, M. L. Molina, J. L. Ayala, E. Montoya, M. L. Renart, A. M. Fernandez, J. A. Encinar, A. V. Ferrer-Montiel, J. A. Poveda, J. M. Gonzalez-Ros, *Biochim. Biophys. Acta Biomembr.* **2013**, *1828*, 193–200.

[8] J. Hegermann, J. Overbeck, H. Schrempf, *Microbiology* **2006**, *152*, 2831–2841.

[9] a) M. Etzkorn, A. Bockmann, A. Lange, M. Baldus, *J. Am. Chem. Soc.* **2004**, *126*, 14746–14751; b) J. Maciejko, M. Mehler, J. Kaur, T. Lieblein, N. Morgner, O. Ouari, P. Tordo, J. Becker-Baldus, C. Glaubitz, *J. Am. Chem. Soc.* **2015**, *137*, 9032–9043.

[10] M. Weingarth, G. Bodenhausen, P. Tekely, *J. Am. Chem. Soc.* **2009**, *131*, 13937–13939.

[11] L. G. Cuello, J. G. Romero, D. M. Cortes, E. Perozo, *Biochemistry* **1998**, *37*, 3229–3236.

[12] A. van Dalen, S. Hegger, J. A. Killian, B. de Kruijff, *FEBS Lett.* **2002**, *525*, 33–38.

[13] D. M. Cortes, E. Perozo, *Biochemistry* **1997**, *36*, 10343–10352.

[14] a) V. S. Bajaj, M. L. Mak-Jurkauskas, M. Belenky, J. Herzfeld, R. G. Griffin, *Proc. Natl. Acad. Sci. USA* **2009**, *106*, 9244–9249; b) T. Jacso, W. T. Franks, H. Rose, U. Fink, J. Broecker, S. Keller, H. Oschkinat, B. Reif, *Angew. Chem. Int. Ed.* **2012**, *51*, 432–435; *Angew. Chem.* **2012**, *124*, 447–450; c) E. J. Koers, E. A. van der Cruijsen, M. Rosay, M. Weingarth, A. Prokofyev, C. Sauvee, O. Ouari, J. van der Zwan, O. Pongs, P. Tordo, W. E. Maas, M. Baldus, *J. Biomol. NMR* **2014**, *60*, 157–168; d) M. A. Voinov, D. B. Good, M. E. Ward, S. Milikisiyants, A. Marek, M. A. Caporini, M. Rosay, R. A. Munro, M. Ljumovic, L. S. Brown, V. Ladizhansky, A. I. Smirnov, *J. Phys. Chem. B* **2015**, *119*, 10180–10190; e) S. Y. Liao, M. Lee, T. Wang, I. V. Sergeyev, M. Hong, *J. Biomol. NMR* **2016**, *64*, 223–237; f) E. Lehnert, J. Mao, A. R. Mehdipour, G. Hummer, R. Abele, C. Glaubitz, R. Tampe, *J. Am. Chem. Soc.* **2016**, *138*, 13967–13974; g) J. Becker-Baldus, C. Bamann, K. Saxena, H. Gustmann, L. J. Brown, R. C. Brown, C. Reiter, E. Bamberg, J. Wachtveitl, H. Schwalbe, C. Glaubitz, *Proc. Natl. Acad. Sci. USA* **2015**, *112*, 9896–9901; h) M. Kaplan, S. Narasimhan, C. de Heus, D. Mance, S. van Doorn, K. Houben, D. Popov-Celeketic, R. Damman, E. A. Katrukha, P. Jain, W. J. C. Geerts, A. J. R. Heck, G. E. Folkers, L. C. Kapitein, S. Lemeer, P. M. P. V. E. Henegouwen, M. Baldus, *Cell* **2016**, *167*, 1241–1251.

[15] M. Weingarth, E. A. van der Cruijsen, J. Ostmeyer, S. Lievestro, B. Roux, M. Baldus, *J. Am. Chem. Soc.* **2014**, *136*, 2000–2007.

[16] E. A. van der Cruijsen, A. V. Prokofyev, O. Pongs, M. Baldus, *Biophys. J.* **2017**, *112*, 99–108.

[17] M. Iwamoto, S. Oiki, *Proc. Natl. Acad. Sci. USA* **2013**, *110*, 749–754.

[18] D. H. de Jong, G. Singh, W. F. D. Bennett, C. Arnarez, T. A. Wassenaar, L. V. Schafer, X. Periole, D. P. Tieleman, S. J. Marrink, *J. Chem. Theory Comput.* **2013**, *9*, 687–697.

[19] a) G. van den Bogaart, K. Meyenberg, H. J. Risselada, H. Amin, K. I. Willig, B. E. Hubrich, M. Dier, S. W. Hell, H. Grubmuller, U. Diederichsen, R. Jahn, *Nature* **2011**, *479*, 552–555; b) X. Periole, A. M. Knepp, T. P. Sakmar, S. J. Marrink, T. Huber, *J. Am. Chem. Soc.* **2012**, *134*, 10959–10965.

[20] E. A. van der Cruijsen, D. Nand, M. Weingarth, A. Prokofyev, S. Hornig, A. A. Cukkemane, A. M. Bonvin, S. Becker, R. E. Hulse, E. Perozo, O. Pongs, M. Baldus, *Proc. Natl. Acad. Sci. USA* **2013**, *110*, 13008–13013.

[21] R. P. Huijbregts, A. I. de Kroon, B. de Kruijff, *Biochim. Biophys. Acta Biomembr.* **2000**, *1469*, 43–61.

[22] S. Uysal, V. Vasquez, V. Tereshko, K. Esaki, F. A. Fellouse, S. S. Sidhu, S. Koide, E. Perozo, A. Kossiakoff, *Proc. Natl. Acad. Sci. USA* **2009**, *106*, 6644–6649.

[23] T. A. Wassenaar, K. Pluhackova, R. A. Bockmann, S. J. Marrink, D. P. Tieleman, *J. Chem. Theory Comput.* **2014**, *10*, 676–690.